Stem Cells Translational Medicine, 2022, **11**, 297–309
https://doi.org/10.1093/stcltm/szab031
Advance access publication 10 March 2022
Original Research

Site-Specific Integration of *TRAIL* in iPSC-Derived Mesenchymal Stem Cells for Targeted Cancer Therapy

Zujia Wang[1], Hongting Chen[1], Peiyun Wang[1], Miaojin Zhou[1], Guangxu Li[1], Zhiqing Hu[1], Qian Hu[1], Junya Zhao[1], Xionghao Liu[1], Lingqian Wu[*,1], Desheng Liang[*,1]

[1]Center for Medical Genetics & Hunan Key Laboratory of Medical Genetics, School of Life Sciences, Central South University, Changsha, Hunan, People's Republic of China

*Corresponding authors: Lingqian Wu, MD, PhD, Professor, Center for Medical Genetics & Hunan Key Laboratory of Medical Genetics, School of Life Sciences, Central South University, 110 Xiangya Road, Changsha, Hunan 410078, People's Republic of China. Tel: +86-731-84805252; Fax: +86-731-84478152; Email: wulingqian@sklmg.edu.cn; Desheng Liang, MD, PhD, Professor, Center for Medical Genetics & Hunan Key Laboratory of Medical Genetics, School of Life Sciences, Central South University, 110 Xiangya Road, Changsha, Hunan 410078, People's Republic of China. Tel: +86-731-84805252; Fax: +86-731-84478152; Email: liangdesheng@sklmg.edu.cn

Abstract

Mesenchymal stem cells (MSCs) are a promising cellular vehicle for transferring anti-cancer factors to malignant tumors. Currently, a variety of anti-cancer agents, including the tumor necrosis factor (TNF)-related apoptosis-inducing ligand (TRAIL), have been loaded into MSCs derived from a range of sources through different engineering methods. These engineered MSCs exhibit enormous therapeutic potential for various cancers. To avoid the intrinsic defects of MSCs derived from tissues and the potential risk of viral vectors, *TRAIL* was site-specifically integrated into the ribosomal DNA (rDNA) locus of human-induced pluripotent stem cells (iPSCs) using a non-viral rDNA-targeting vector and transcription activator-like effector nickases (TALENickases). These genetically modified human iPSCs were differentiated into an unlimited number of homogeneous induced MSCs (TRAIL-iMSCs) that overexpressed TRAIL in both culture supernatants and cell lysates while maintaining MSC-like characteristics over continuous passages. We found that TRAIL-iMSCs significantly induced apoptosis in A375, A549, HepG2, and MCF-7 cells in vitro. After intravenous infusion, TRAIL-iMSCs had a prominent tissue tropism for A549 or MCF-7 xenografts and significantly inhibited tumor growth through the activation of apoptotic signaling pathways without obvious side effects in tumor-bearing mice models. Altogether, our results showed that TRAIL-iMSCs have strong anti-tumor effects in vitro and in vivo on a range of cancers. This study allows for the development of an unlimited number of therapeutic gene-targeted MSCs with stable quality and high homogeneity for cancer therapy, thus highlighting a universal and safe strategy for stem cell-based gene therapy with high potential for clinical applications.

Keywords: cancer; induced pluripotent stem cells; mesenchymal stem cells; gene targeting; cellular therapy

Graphical Abstract

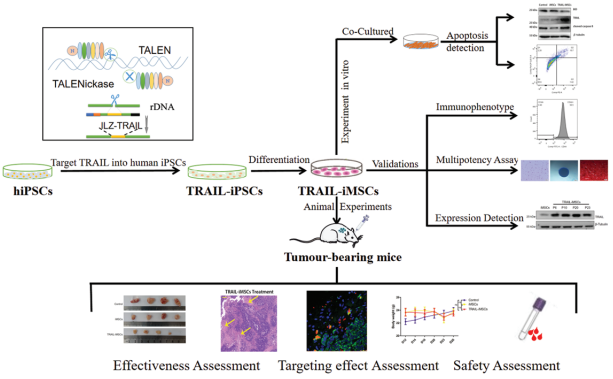

Significance Statement

Induced pluripotent stem cell (iPSC)-derived mesenchymal stem cells (iMSCs) hold promise for cancer treatment. The significance of this study is the generation of tumor necrosis factor-related apoptosis-inducing ligand (TRAIL)-iMSCs by non-viral gene targeting of iPSCs that have the capacity to induce apoptosis of tumor cells and suppress the growth of tumor xenografts. In addition to generating a potential therapeutic cell source for cancer treatment, this study highlights the persistent expression of therapeutic genes and high proliferative capacity of iMSCs over continuous passages, showing a major advantage over other MSC sources and great potential for clinical applications.

Received: 10 August 2021; Accepted: 22 November 2021.

Introduction

Recent preclinical and clinical studies of cancer therapy show great promise for cell-based therapeutic strategies. Certain types of stem cells have been increasingly considered as tumor-specific delivery vehicles to treat a number of different cancer types. Among them, mesenchymal stem cells (MSCs) have become the most frequently used stem cell type in the clinical setting because of their numerous advantages.[1-3] The tropism, engraftment, and proliferation of MSCs at the sites of primary tumors and their metastases have allowed the development of a potential cellular vehicle for the delivery of anti-cancer effectors to malignant cells. Both naïve (unmodified) and modified MSCs (used as tumor-specific delivery vehicles for therapeutic compounds, suicide genes, therapeutic genes, and oncolytic viruses) have been used in in vitro and in vivo cancer models.[4]

Engineered MSCs expressing tumor necrosis factor (TNF)-related apoptosis-inducing ligand (TRAIL) have emerged as a platform for effective and targeted cancer treatment. TRAIL, also known as Apo2L, CD253, and TNFSF10, is a member of the TNF superfamily. Because TRAIL is capable of preferentially inducing apoptosis in tumor cells through the activation of specific agonistic receptors (DR4/DR5) but has no toxic effect on normal cells, it offers exciting prospects as a cancer therapeutic method.[5,6] TRAIL can induce cell death via caspase-8 activation and initiate extrinsic and/or intrinsic pathways while activating various apoptotic signaling molecules.[7] *TRAIL*-engineered MSCs are able to directly home-in on the tumor microenvironment and exert anti-cancer activity efficiently in a wide range of cancers,[8,9] thus garnering considerable interest as a viable therapeutic strategy. An increasing number of studies of loading *TRAIL* to MSCs using viral vectors have shown effectiveness.[10-12] However, there are many obstacles that are significantly hampering the clinical application of genetically modified tissue-derived MSCs,[13] including difficult and invasive access methods, cell population heterogeneity, insufficient and non-persistent expression of therapeutic genes, potential risk of viral insertion, and loss of pluripotency and proliferative capacities over continuous passages.

An unlimited, cost-effective source of MSCs would be a better candidate for autologous MSC transplantation. In addition, a reliable candidate site for transgene integration and long-term expression is crucial for therapeutic outcomes. Recent studies have shown that induced pluripotent stem cells (iPSCs) can be harnessed to generate a limitless source of MSCs that can be applied as autologous cells in cancer therapy.[13-15] To achieve safe, stable, and effective expression of TRAIL in MSCs, we designated the ribosomal DNA (rDNA) locus as a transgenic site and obtained a large number of therapeutic-induced MSCs (iMSCs) through directional differentiation after acquiring genetically modified iPSCs.

There are 600-800 copies of the ribosomal DNA (rDNA) gene with high transcriptional activity and property of increased recombinational rate in the human genome. Such a large number of copies provide plentiful recombination sites for homologous recombination,[16,17] which guarantees high expression of TRAIL after site-specific integration. Previously, we successfully targeted IL-24 in the rDNA locus of iPSCs (IL-24-iPSCs) and found that the IL-24-iMSCs derived from IL-24-iPSCs significantly inhibited the growth of melanoma cells in vitro and in tumor-bearing mouse models.[18,19]

In this study, by taking advantage of integrating and expressing multiple copies of exogenous genes efficiently at the rDNA locus, we targeted a non-viral vector (minipHrneo-ILZ-sTRAIL) containing *TRAIL* in the rDNA locus with the help of transcription activator-like effector nickase (TALENickase).[20] Furthermore, an unlimited number of therapeutic homogeneous TRAIL-iMSCs from genetically modified TRAIL-iPSCs were generated for in vitro and in vivo anti-tumor effect studies and exhibited promising results when inducing cell apoptosis and tumor growth suppression for a range of cancers. This strategy has the advantage of providing unlimited sources of MSCs with stable quality, high homogeneity, and relatively controllable therapeutic properties to meet the individual needs of patients, thereby hopefully overcoming the existing barriers to clinical applications.

Materials and Methods

Cell Culture

Human iPSCs (hiPSCs), which were previously reprogrammed from exfoliated renal tubular epithelial cells (urine cells) with episomes by our group, were cultured in mTeSR1 medium (STEMCELL Technologies, Vancouver, BC, Canada). Every 3-4 days, hiPSCs were passaged with 0.5 mM EDTA (Thermo Fisher Scientific, Waltham, MA, USA) and plated onto fresh Matrigel-coated dishes (Matrigel, BD Biosciences, Bedford, MA, USA). Four types of human cancer cell lines (A375, A549, MCF-7, and HepG2) purchased from the American Type Culture Collection (Manassas, VA, USA) were cultured in DMEM/high glucose (HyClone, Logan, UT, USA) supplemented with 10% fetal bovine serum (Gibco, Carlsbad, CA, USA). The iMSCs derived from hiPSCs were cultured in MSC medium with DMEM/low glucose (HyClone) supplemented with 10% fetal bovine serum (Gibco) and 10 μg/mL basic fibroblast growth factor (Sigma-Aldrich, St. Louis, MO, USA). All the cells were maintained in disposable sterile dishes or flasks (Corning, NY, USA) and passaged or harvested when they reached 80%-90% confluence. All cells were grown at 37°C in a humidified atmosphere containing 5% CO_2. Mycoplasma testing was performed and all human cell lines were authenticated using STR profiling within the past 3 years.

Construction of minipHrneo-ILZ-sTRAIL Plasmid and Transformation of hiPSCs

The targeting vector construct and homologous recombination-based targeting scheme are summarized in Fig. 1A. In our previous study,[18] we constructed a non-viral human rDNA (hrDNA) targeting vector, called minipHrneo, containing a non-promoter neomycin (Neo) cassette flanked by a pair of loxP sequences. In this study, we inserted a cytomegalovirus promoter-driven ILZ-sTRAIL (isoleucine zipper and short TRAIL fusion protein) expression cassette into the suitable restriction site of minipHrneo to generate minipHrneo-ILZ-sTRAIL. The final product was sequenced by Sanger sequencing. All restriction endonucleases were purchased from New England Biolabs (Beverly, MA, USA). All reaction kits for the polymerase chain reaction (PCR) and ligation were purchased from Takara Bio (Shiga, Japan).

For gene targeting, hiPSCs were dissociated into a single-cell suspension with TrypLE Select (Invitrogen, Carlsbad, CA, USA) at 37°C for 3 minutes, harvested, and counted. After

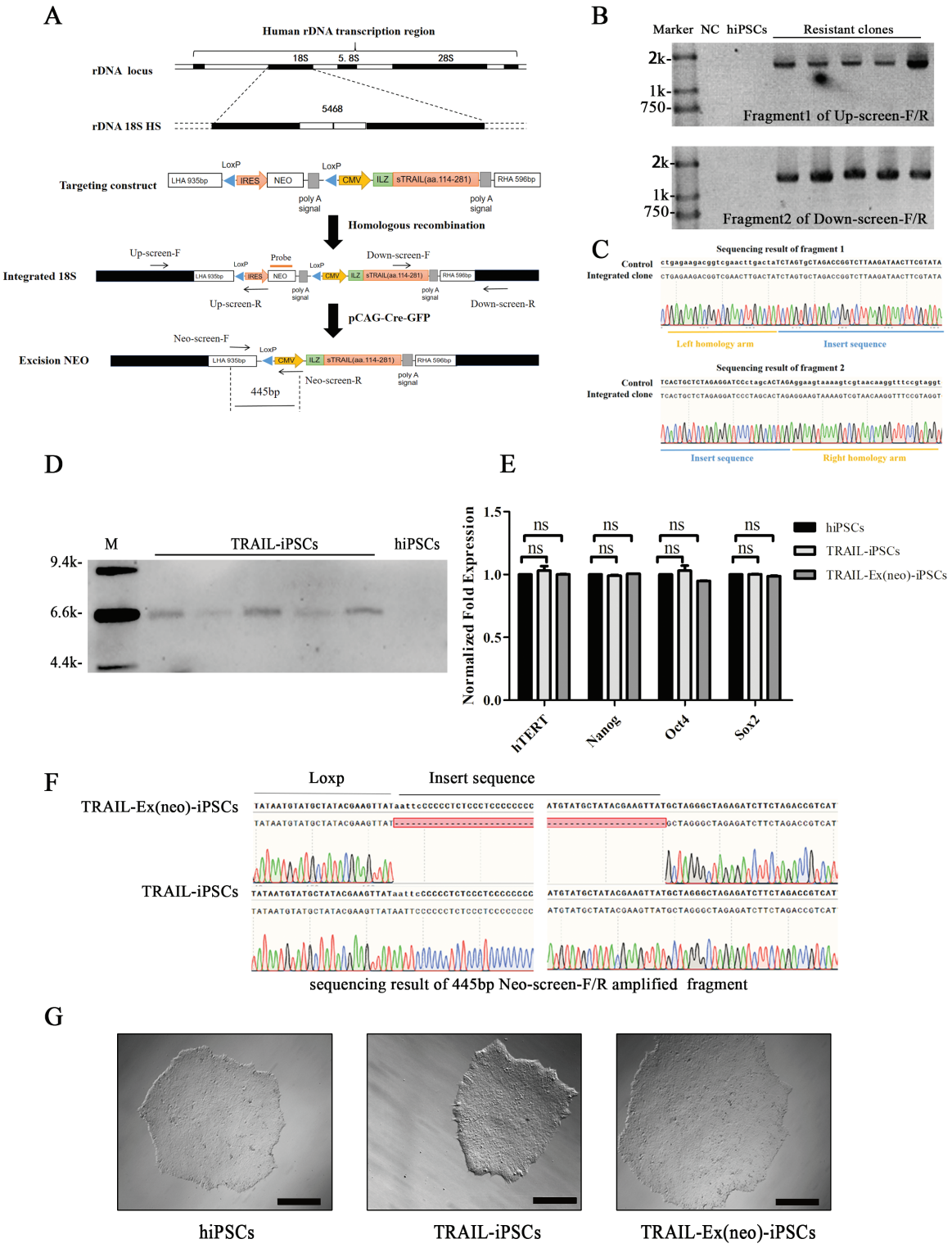

Figure 1. Analysis of site-specific integration of ILZ-sTRAIL at the rDNA locus of hiPSCs. (A) Schematic diagram of rDNA targeting vector minipHrneo-ILZ-sTRAIL and gene targeting process flowcharts. The 935-bp left homologous arm (LHA) (GenBank U13369: 4533-5467) and 596-bp right homologous arm (RHA) (GenBank U13369: 5468-6064) are shown by white boxes. The neomycin cassette consists of an IRES element, the coding region of the neomycin gene (NEO), and SV40 polyA signal, flanked by a pair of 34-bp loxP sequences (triangles). The ILZ-sTRAIL gene is driven by a cytomegalovirus (CMV) promoter. Binding sites of primers Up-screen-F/R and Down-screen-F/R are indicated. Neo-screen-F/R for identification of neomycin removal bind outside of the deletion region. (B) G418-resistant iPSCs clones were screened for homologous recombination by PCR with Up-screen-F/R and Down-screen-F/R which would generate 1652-bp and 1492-bp PCR products, respectively, if the cells underwent homologous recombination. (C) Tow PCR products were further verified by Sanger sequencing. Both fragments were consistent with the expected theoretical sequences. (D) Clones that had achieved homologous recombination at the rDNA locus (based on PCR) were verified by Southern blotting analysis with a 358-bp DIG-probe designed within the Neo cassette, XhoI digesting genomic DNA yielded expected 6.5k restriction fragments. (E) Relative transcription levels of pluripotent factors (hTERT, Nanog, Oct-4, and Sox-2) in hiPSCs, TRAIL-iPSCs, TRAIL-Ex(neo)-iPSCs were detected by qRT-PCR (data are mean ± SEM, $n = 3$ for each group, two-way ANOVA). (F) Sanger sequencing to confirm the Neo cassette precise excisions in pCAG-Cre-GFP transfected TRAIL-iPSCs. (G) Morphology of

centrifugation, 3 × 10^6 cells were re-suspended in 100 µL of Human Stem Cell Nucleofector Kit 2 solution (Lonza, Basel, Switzerland) with 5 µg of minipHrneo-ILZ-sTRAIL and 5 µg of TALEN/TALENickases, as previously described.[18,20] Nucleofection was completed using program B-016 on Nucleofector II (Lonza). Transfected cells were maintained in Matrigel-coated dishes with mTeSR1 medium supplemented with 10% Clone R (STEMCELL Technologies). On the third day after transfection, a final concentration of 50 µg/mL G418 (Sigma-Aldrich) was added to the culture medium for 6 days to select integrated hiPSCs. Then, the G418-resistant clones were picked manually and expanded for subsequent identification and use.

Excision of Neo Cassettes

To excise the Neo cassette, 2 µg of the Cre recombinase-expressing vector pCAG-Cre-GFP was transfected using Lipofectamine (Invitrogen) in 1 × 10^6 integrated TRAIL-iPSCs. The next day, the transfected cells were cultured at a density of 2 × 10^3 cells/6-cm dish with mTeSR1 medium supplemented with 10% CloneR (STEMCELL Technologies) for 10 days; then, the standalone TRAIL-iPSC clones were picked manually and expanded for subsequent identification and use.

Identification of Site-Specific Integration TRAIL-iPSCs Colonies

The G418-resistant hiPSCs colonies were identified through PCR, Sanger sequencing, and Southern blotting. The pCAG-Cre-GFP-transfected TRAIL-iPSC clones were identified by PCR and Sanger sequencing.

Genomic DNA was isolated from iPSCs using the standard phenol/chloroform extraction method. PCR was performed using LA Taq DNA polymerase (TaKaRa) according to the manufacturer's instructions. Pairs of primers, Up-screen-F/Up-screen-R and Down-screen-F/Down-screen-R, which both have an annealing temperature of 60°C, were used to identify the site-specific integration colonies. To identify the Neo cassette-excised TRAIL-iPSCs colonies, the primers Neo-screen-F/Neo-screen-R (57°C) were used, and the PCR product length of the Neo cassette-excised TRAIL-iPSC clones was 445 bp. All PCR products were identified by Sanger sequencing. The primer sequences are listed in Supplementary Table S2.

Southern blotting was conducted to exclude non-directed integration clones as follows: 10 µg of genomic DNA was digested with XhoI restriction enzyme (New England Biolabs) overnight and then electrophoresed on a 0.8% agarose gel for 3 hours at 120 V. Digested DNA fragment transfer was performed overnight onto a positively charged nylon membrane by capillary blotting in 0.4 M NaOH (nylon membrane; Roche Diagnostics, Basel, Switzerland). DIG-labeled λ-HindIII DNA Marker (Roche Diagnostics) was used as the molecular weight marker. The blots on the nylon membrane were hybridized with DIG-dUTP-labeled probes overnight at 42°C. After incubation with the AP-conjugated DIG antibody (Roche Diagnostics) and washing, the signals were measured using CDP-Star (Roche Diagnostics) as a chemiluminescent substrate. Probes were generated using a PCR DIG Probe Synthesis Kit (Roche Diagnostics) with the probe-F/R primers (listed in Supplementary Table S2). The length of the probes was 358 bp (the positions of the probes are mapped in Fig. 1A).

Karyotyping

hiPSCs, site-specific integration TRAIL-iPSCs, and Neo cassette-excised TRAIL-iPSCs cells were treated with 0.08 µg/mL colcemid (Sigma-Aldrich) for 2.5 hours. Subsequently, the cells were trypsinized, centrifuged, and exposed to 0.075 M KCl at 37°C for 30 minutes, fixed with Carnoy's fixative (3:1 methanol:acetic acid; Sinopharm Chemical Reagent, Shanghai, China). Metaphase chromosome spreads were prepared according to standard procedures using air-drying. Karyotyping was evaluated with Giemsa Trypsin banding staining using standard techniques.

Generation and Characterization of MSCs Derived from iPSCs

For the differentiation of iPSCs into iMSCs, we used the STEMdiff Mesenchymal Progenitor Kit (STEMCELL Technologies) following the manufacturer's protocol. Briefly, iPSCs were cultured to 40%-50% confluence on Matrigel-coated plates in mTeSR1 medium. Then, they were cultured in mesenchymal induction medium for 4 days and, subsequently, in MesenCult-ACF medium for 2 days. During the induction period of iPSCs into MSCs, the medium was changed daily. Next, cells were passaged onto a six-well plate pre-coated with the MesenCult-ACF attachment substrate, and the MesenCult-ACF medium was changed every 2 days. Cells that reached 90% confluence were passaged onto a 6-cm dish pre-coated with the MesenCult-ACF attachment substrate and cultured in MesenCult-ACF medium. After continuous culture until passage 5, MSC-like cells were seeded in gelatin-coated plates and cultured in MSC medium.

To identify the surface antigens expressed by iMSCs, the cell suspension was prepared at a concentration of 1 × 10^6 cells/mL in 1 × Dulbecco's phosphate-buffered saline with 5% fetal bovine serum (Gibco). Cells (1 × 10^5) were incubated with BV421-conjugated anti-human CD34/CD45/HLA-DR, BB515-conjugated anti-human CD44, PrecpCy5.5-conjugated anti-human CD73, APC-conjugated anti-human CD105, and PE-Cy7-conjugated anti-human CD90 (BD Biosciences) at room temperature for 20 minutes. Stained cells were washed twice with ice-cold 1 × Dulbecco's phosphate-buffered saline. Flow cytometric analysis was performed using a flow cytometer (BD Biosciences) to detect the expression of cell surface markers on iMSCs, TRAIL-iMSCs, and hiPSCs.

The tri-lineage differentiation potential of iMSCs was identified through osteogenesis, adipogenesis, and chondrogenesis differentiation. Differentiation of adipocytes, osteocytes, and chondrocytes was performed using the StemPro Osteogenesis Differentiation Kit (Gibco), MesenCul Adipogenic Differentiation Kit (STEMCELL Technologies), and MesenCult ACF Chondrogenic Differentiation Kit (STEMCELL Technologies) according to the manufacturer's protocols. Following differentiation culture for 2-3 weeks,

representative hiPSCs, TRAIL-iPSCs, TRAIL-Ex(neo)-iPSCs clones (scale bar = 500 µm). Abbreviations: hiPSCs, human-induced pluripotent stem cells; IRES, internal ribosomal entry site; PCR, polymerase chain reaction; qRT-PCR, quantitative reverse transcription polymerase chain reaction; rDNA, ribosomal DNA; TRAIL, tumor necrosis factor-related apoptosis-inducing ligand.

cells were stained with an appropriate amount of Alizarin Red, Oil Red O, or Alcian blue dye for 30 minutes. After incubation and washing, stained cells were analyzed using a light microscope.

Real-Time Quantitative Polymerase Chain Reaction

Total RNA was extracted using Trizol reagent (Sigma-Aldrich) and subsequently treated with DNase I (Thermo Fisher Scientific) to eliminate gDNA and other DNA contamination. Then, 500 ng of the total RNA sample was reverse-transcribed using HiScript II Q RT SuperMix (Vazyme, China). Quantitative PCR was performed using the ChamQ Universal SYBR quantitative PCR Master Mix (Vazyme) on a Bio-Rad CFX96 Touch quantitative PCR System (Bio-Rad, Hercules, CA, USA) according to the manufacturer's instructions. Data analysis was performed using Bio-Rad CFX Manager software (Bio-Rad).

Primers sTRAIL-rtF/R were designed to amplify TRAIL mRNA. β-actin was used as an internal control gene with the β-actin-rtF/R primers.

To assess the expression of pluripotent factors in iPSCs, 5 genes, hTERT, Nanog, Oct-4, and Sox-2 as pluripotency markers and the housekeeping gene HPRT as a control, were amplified using a standard protocol. The sequences of the primers are listed in Supplementary Table S2.

Cell Proliferation Assay

TRAIL-iMSCs were plated on six-well plates at 1×10^5 cells/well and MSC medium was refreshed every day. Every day for 6 days, the cells in each well were harvested and cell numbers were counted. The cumulative cell numbers were calculated and plotted.

Enzyme-Linked Immunosorbent Assay

hiPSCs, TRAIL-iPSCs, bone marrow MSCs, iMSCs, and TRAIL-iMSCs were seeded in six-well plates for 24 hours. Supernatants were collected and total cells were trypsinized and counted. Enzyme-linked immunosorbent assays were performed using the Human TRAIL/TNFSF10 Immunoassay enzyme-linked immunosorbent assay kit (R&D Systems, Minneapolis, MN, USA) according to the manufacturer's instructions.

Western Blotting for Detection of TRAIL

Total cell lysates from hiPSCs, TRAIL-iPSCs, iMSCs, and TRAIL-iMSCs were prepared using RIPA lysis buffer (Beyotime, Shanghai, China) and quantified using the Pierce BCA Protein Assay Kit (Thermo Fisher Scientific). Cell lysate samples (10 μg) were loaded for electrophoresis by SDS-PAGE and transferred to poly(vinylidene fluoride) (PVDF) membranes (Millipore, Bedford, MA, USA). After blocking with 5% bovine serum albumin in 0.1% Tris-buffered saline with Tween, membranes were incubated overnight with the primary anti-human TRAIL antibody (1:1000, ab42121; Abcam, Cambridge, MA, USA) and the anti-human β-actin antibody (1:10 000, A1978; Sigma-Aldrich) at 4°C. The next day, membranes were thoroughly washed and incubated with the horseradish peroxidase-conjugated anti-rabbit (1:10 000; Jackson ImmunoResearch, West Grove, PA, USA) and anti-mouse secondary antibodies (1:10 000; Jackson ImmunoResearch) for 1 hour at room temperature. Finally, protein signals were detected with an enhanced chemiluminescence kit (SuperSignal West Femto Maximum Sensitivity Substrate; Thermo Fisher Scientific) using a Bio-Rad imaging system according to the manufacturer's instructions. Pre-stained molecular weight standards (Thermo Fisher Scientific) were used to estimate the apparent molecular weights.

Apoptosis Detection

To validate the ability of iMSCs to induce cell apoptosis, iMSCs and TRAIL-iMSCs were labeled with the CFSE Cell Division Tracker Kit (Biolegend, San Diego, CA, USA) to distinguish them from tumor cells. Then, 1×10^5 cancer cells (A375, A549, MCF-7, and HepG2) and 3×10^5 CFSE-labeled iMSCs or TRAIL-iMSCs were cocultured in six-well plates with MSC medium. Tumor cells cultured alone served as negative controls. The plates were incubated at 37°C with 5% CO_2. Cells from each group were harvested after 72 hours of coculturing and stained with Annexin V-PE/7-AAD Apoptosis Detection Kit (Vazyme) according to the manufacturer's instructions. Then, flow cytometric analysis was performed to estimate the percentage of apoptotic cancer cells (ie, CFSE-negative, Annexin V-positive).

Animal Experiments

Four-week-old male BALB/cByJ nude mice were purchased from Hunan Slack Scene of Laboratory Animal Company (certificate no. SCXK [Xiang] 2019-0004; Changsha, China). The mice were kept in standard boxes in a room with controlled light and temperature under specific pathogen-free conditions. All animal studies were approved in advance by the Animal Ethics and Experimentation Committee of the School of Life Sciences, Central South University. For subcutaneous xenograft mouse models, 5×10^6 cancer cells (A375 or MCF-7) were subcutaneously implanted in the back of each mouse (each treatment group included at least 6 mice).

TRAIL-iMSCs and iMSCs were labeled with 10 μM CM-Dil (Invitrogen) according to the manufacturer's instructions. Labeled cells were washed with Dulbecco's phosphate-buffered saline and cultured in MSC culture medium. Labeling efficiency was examined using a fluorescent microscope. Two weeks after the establishment of the tumor model, 3×10^6 CM-Dil-labeled iMSCs or TRAIL-iMSCs were implanted into the tumor-bearing mice by retro-orbital intravenous injection under anesthesia. The weight of the mice and the diameters of the tumor sizes (including length and width) were measured at regular intervals. The tumor volumes were calculated according to the following formula: tumor volume (mm^3) = (length × $width^2$)/2. The growth curve of the tumor was drawn accordingly.

Immunofluorescence and Histological Analysis

Heavily anesthetized mice were sacrificed by cervical dislocation within 4 weeks of the xenograft. Tumor tissues were collected, photographed, and analyzed. Harvested tumor tissues were fixed with 4% paraformaldehyde and used for frozen sections (thickness, 15 μm) or paraffin sections (thickness, 10 μm). Frozen sections were incubated with anti-human TRAIL antibody (1:200, 27064-1-AP; Proteintech, Wuhan, China), followed by incubation with fluorescent anti-rabbit AF488 secondary antibody (Thermo Fisher Scientific). Nuclei were stained with DAPI (Sigma-Aldrich). CM-Dil-labeled iMSCs and fluorescence staining of TRAIL were visualized and acquired by confocal fluorescence microscopy (Leica, Wetzlar, Germany). Paraffin sections were stained with hematoxylin

and eosin for histological examination. Five visual fields for each group were randomly assessed during the statistical analysis of the percentage of necrotic/vacuolated area in the tumor tissue. The area was quantified using ImageJ software.

Western Blotting for the Detection of Apoptosis-Related Factors

Cocultured cancer cells or tumor tissues were prepared using RIPA lysis buffer (Beyotime) and quantified using the Pierce BCA Protein Assay Kit (Thermo Fisher Scientific).

For each sample, 10 μg of protein lysate was loaded onto 12% SDS-PAGE (Invitrogen) for electrophoresis and immunoblotting. After blocking, PVDF membranes were incubated with the primary anti-human TRAIL antibody (1:1000; ab42121; Abcam), anti-human caspase-3 antibody (1:1000, #9661; CST, Boston, MA, USA), anti-human caspase-8 antibody (1:1000, 13423; Proteintech), anti-human cleaved PARP-1 antibody (1:1000, sc-56196; Santa Cruz, CA, USA), anti-human BID antibody (1:1000, #2002; CST), anti-human BAX antibody (1:1000, sc-7480; Santa Cruz), and anti-β-tubulin antibody (1:10 000, T4026; Sigma-Aldrich) overnight at 4°C. PVDF membranes were washed and incubated with horseradish peroxidase-conjugated secondary antibodies (1:10 000; Jackson ImmunoResearch) for 1 hour at room temperature, and blots were detected using an enhanced chemiluminescence kit (Thermo Fisher Scientific). Pre-stained molecular weight standard markers (Thermo Fisher Scientific) were used to estimate the apparent molecular weights.

Statistical Analysis

All experiments were performed independently at least 3 times, and triplicates were performed for each condition or group. A one-way analysis of variance and two-way analysis of variance were used to analyze the data of different experimental groups using GraphPad 5.0 software. Data are expressed as mean ± standard error of the mean. Statistical significance was set at $P < .05$.

Results

Construction of Non-Viral Gene-Targeting Vector minipHrneo-ILZ-sTRAIL

We constructed the optimized rDNA-targeting vector minipHrneo-ILZ-sTRAIL (Fig. 1A) to target the ILZ-sTRAIL (isoleucine zipper and short TRAIL fusion protein) expression cassette in the rDNA locus. The minipHrneo-ILZ-sTRAIL contained 2 cassettes. One cassette was a promoter-less Neo cassette flanked by a pair of 34-bp loxP sequences (triangles) containing an encephalomyocarditis virus internal ribosomal entry site (EMCV-IRES), which enabled gene transcription under the control of the upstream endogenous RNA polymerase I promoter, and loxP sequences, which facilitated the subsequent removal of the neo screening genes. The other cassette was a cytomegalovirus enhancer and promoter driving the ILZ-sTRAIL expression cassette. The 2 cassettes were flanked by a long left homologous arm (935 bp) and a short right homologous arm (596 bp) of the target site. The vector plasmid was confirmed using Sanger sequencing.

Targeting of ILZ-sTRAIL in rDNA Locus in hiPSCs

A total of 5 of 12 G418-resistant strains were identified as homologous recombination by PCR amplification, which generated 1652-bp and 1492-bp PCR products, respectively (Fig. 1B). Sanger sequencing revealed that the PCR products were consistent with expectations, suggesting the correct targeting of the exogenous genes (Fig. 1C). Southern blotting analysis showed a single 6.5 kb-restriction fragment, as expected, further confirming that the 5 transformed hiPSC clones carried the target transgene without other site-directed integration (Fig. 1D).

Next, the Cre recombinase-expressing vector pCAG-Cre-GFP was transfected to integrated TRAIL-iPSCs to remove the screening genes (neo). Sequencing of the PCR products revealed that 7 of 10 TRAIL-iPSC clones with the Neo cassette were successfully excised. Figure 1F shows one of these Neo cassette-excised TRAIL-iPSC clones.

The site-specific integrated TRAIL-iPSCs clones and Neo cassette-excised TRAIL-Ex(neo)-iPSCs shared the same morphology and maintained the same gene expression levels of hTERT and other ES-related genes as control hiPSCs (Fig. 1E, 1G).

Characterization of Transcription and Expression Levels of TRAIL-iPSCs

Karyotype analysis of metaphase chromosomes for the TRAIL-iPSC clones and TRAIL-Ex(neo)-iPSC clones showed that their karyotypes were normal and consistent with those of hiPSCs (Fig. 2A). The off-target analysis performed using PCR amplicon sequencing revealed no genome editing in any of the 3 top-ranked off-target sites (Supplementary Fig. S1). These results provide supporting evidence for the safety of our non-viral gene-targeting system for hiPSCs.

The transcript levels of *TRAIL* mRNA of all transformed TRAIL-iPSCs were significantly higher than those of control hiPSCs, with values ranging from 450-fold to 2000-fold (Fig. 2B). The differences observed at the transcription level were likely attributable to the number of insertion copies. Because TRAIL exhibited the highest expression levels in TRAIL-iPSCs-6, we chose these cells for subsequent experiments. Additionally, excision of the Neo cassette did not alter the transcription level of *TRAIL* mRNA in TRAIL-Ex(neo)-iPSCs without neo transcription (Fig. 2C). Furthermore, a quantitative analysis showed that TRAIL protein expression in integrated TRAIL-iPSCs was increased 3-fold to 4-fold compared to that in control hiPSCs, which was consistent with the transcription trends (Fig. 2D, 2E).

Generation and Characterization of iMSCs Derived from TRAIL-iPSCs and hiPSCs

iMSCs were successfully obtained from TRAIL-iPSCs and hiPSCs (Fig. 3A). Our results revealed that TRAIL-iMSCs, iMSCs, and bone marrow MSCs showed a typical spindle-shaped, fibroblast-like morphology (Fig. 3B). Even TRAIL-iMSCs at passage 23 showed no marked aging or de-differentiated shape, thus retaining their cellular characteristics (Fig. 3B; Supplementary Fig. S2). However, tissue-derived MSCs may lose their multipotency and proliferative capacity and undergo changes in cellular plasticity over continuous passages.[21]

Flow cytometric data analysis indicated that the MSC markers CD44, CD73, CD90, and CD105 were expressed by the majority of iMSCs (>95%), whereas the negative MSC markers CD34, CD45, and HLA-DR were expressed by a very small fraction of these cells (<5%). These markers

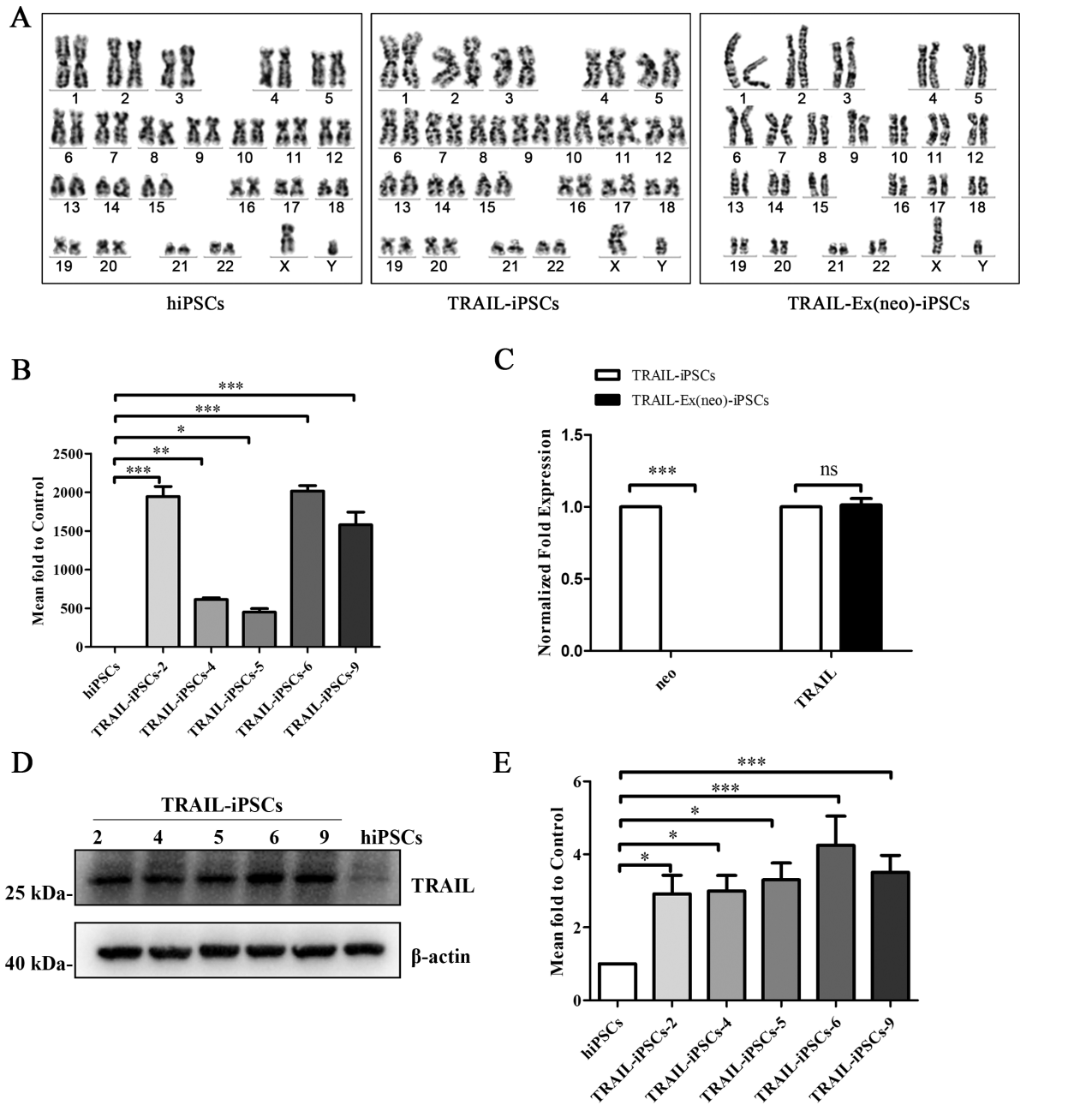

Figure 2. Characterization of TRAIL-iPSCs. (A) G banding karyotype analysis of TRAIL-iPSCs clones and Neo cassette excised TRAIL-iPSCs clones showing a normal karyotype (46, XY) consistent with the normal hiPSCs. (B) Detection of TRAIL mRNA transcription levels in transformed hiPSCs lines (TRAIL-iPSCs-2/4/5/6/9) and control hiPSCs by qRT-PCR. The TRAIL mRNA levels in targeted TRAIL-iPSCs were ~500- to 2000-fold higher than control iPSCs (data are mean ± SEM, $n = 3$ for each group, $^{*}P < .05$, $^{**}P < .01$, $^{***}P < .001$, one-way ANOVA). (C) Neo and TRAIL mRNA relative expression of Neo cassette excised TRAIL-iPSCs clones were quantified by qRT-PCR compared with TRAIL-iPSCs. Excising of Neo cassette without affecting the TRAIL transcription (data are mean ± SEM, $n = 3$ for each group, $^{***}P < .001$, two-way ANOVA). (D and E) TRAIL expression in cell lysates of TRAIL-iPSCs and control hiPSCs clones was analyzed by Western blotting. The protein expression level of TRAIL in the 5 transformed clones was about 3- to 4-fold higher than in control hiPSCs (data are mean ± SEM, $n = 3$ for each group, $^{*}P < .05$, $^{***}P < .001$, one-way ANOVA). Abbreviations: ANOVA, analysis of variance; hiPSCs, human-induced pluripotent stem cells; qRT-PCR, quantitative reverse transcription-polymerase chain reaction; TRAIL, tumor necrosis factor-related apoptosis-inducing ligand.

were significantly different from those of hiPSCs (Fig. 3C) but similar to those of bone marrow MSCs (Supplementary Fig. S3). The assessed multipotency of iMSCs was in accordance with the differentiation of MSCs from the bone marrow (Fig. 3D). These results demonstrated that TRAIL-iMSCs and iMSCs displayed typical characteristics of MSCs, thus fulfilling the basic criteria to be identified as MSCs.[22]

TRAIL-iMSCs Overexpressed Exogenous TRAIL

The cumulative cell numbers of TRAIL-iMSCs over time showed robust proliferation ability in vitro, even until passage 22 (Fig. 3E). Different generations of TRAIL-iMSCs maintained the ability to continuously express the transgene protein TRAIL, which was at least approximately 5-fold more than that of iMSCs (Fig. 3F, 3G).

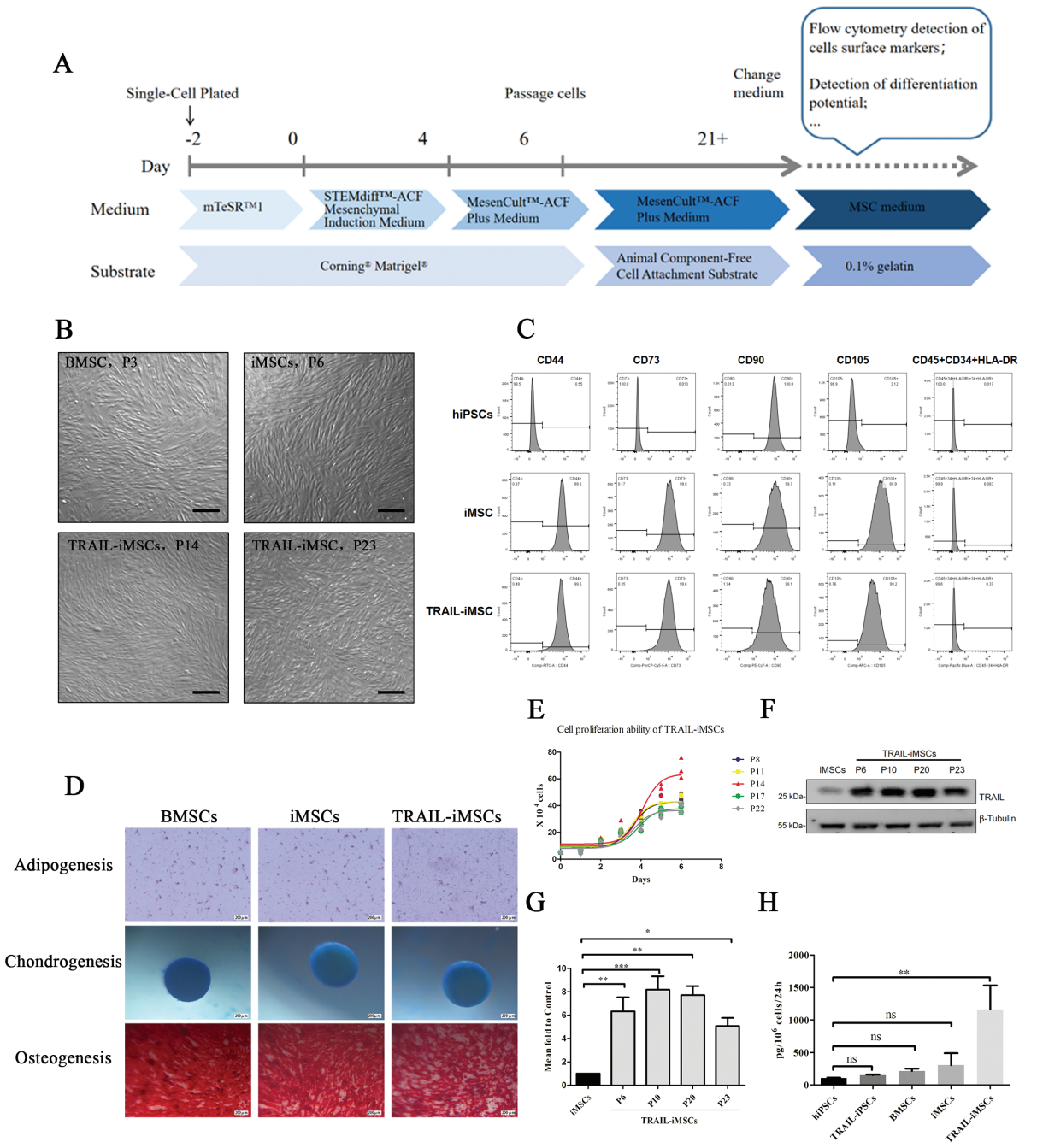

Figure 3. Generation and characterization of iMSCs. (A) Flowcharts of iMSCs differentiation procedure. (B) Morphology of the iMSCs derived from TRAIL-iPSCs and control hiPSCs at different generations vs BMSCs (scale bar = 250 μm). (C) Flow cytometric analysis for detection of iMSCs and TRAIL-iMSCs surface markers CD44, CD73, CD90, CD105, CD34, CD45, and HLA-DR, compared with hiPSCs. (D) Multipotency assays of iMSCs were characterized with differentiation toward adipogenic, osteogenic, and chondrogenic lineage in vitro. The osteogenic cultures were stained with Alizarin Red S to detect calcium deposition. The chondrogenic induced pellets were stained with Alcian blue dye to detect proteoglycans. The adipogenic cultures were stained with Oil Red O to measure the accumulation of lipid droplets (scale bar = 200 μm). (E) Cumulative cell numbers of TRAIL-iMSCs at different generations were calculated and plotted by counting every day. (F and G) Western blotting analysis of cell lysates from TRAIL-iMSCs at different generations compared with iMSCs. The expression levels of TRAIL in TRAIL-iMSCs were about 5- to 8-fold higher than in control iMSCs (data are mean ± SEM, $n = 3$ for each group, $*P < .05$, $**P < .01$, $***P < .001$, one-way ANOVA). (H) ELISA analysis of TRAIL protein in supernatants of hiPSCs, TRAIL-iMSCs, BMSCs, iMSCs, and TRAIL-iMSCs in 1 × 106 cells in 24 hours (data are mean ± SEM, $n = 3$ for each group, $**P < .01$, one-way ANOVA). Abbreviations: hiPSCs, human-induced pluripotent stem cells; iMSCs, induced mesenchymal stem cells; TRAIL, tumor necrosis factor-related apoptosis-inducing ligand; BMSCs, bone marrow mesenchymal stem cells.

TRAIL protein expression in TRAIL-iMSCs was 744-1901 pg/10^6 cells at 24 hours compared to ~300 pg/10^6 cells in control iMSCs and ~100 ng/10^6 cells in TRAIL-iPSCs (Fig. 3H). Moreover, when iPSCs were induced to differentiate into iMSCs, the protein abundance of TRAIL was significantly higher in iMSCs.

Effects of TRAIL-Engineered iMSCs on Tumor Cell Viability In Vitro

Before performing our coculture experiments, we first examined the cytotoxic effects of recombinant human TRAIL. Four tumor cell lines (A375, A549, MCF-7, and HepG2) were confirmed to be sensitive to recombinant

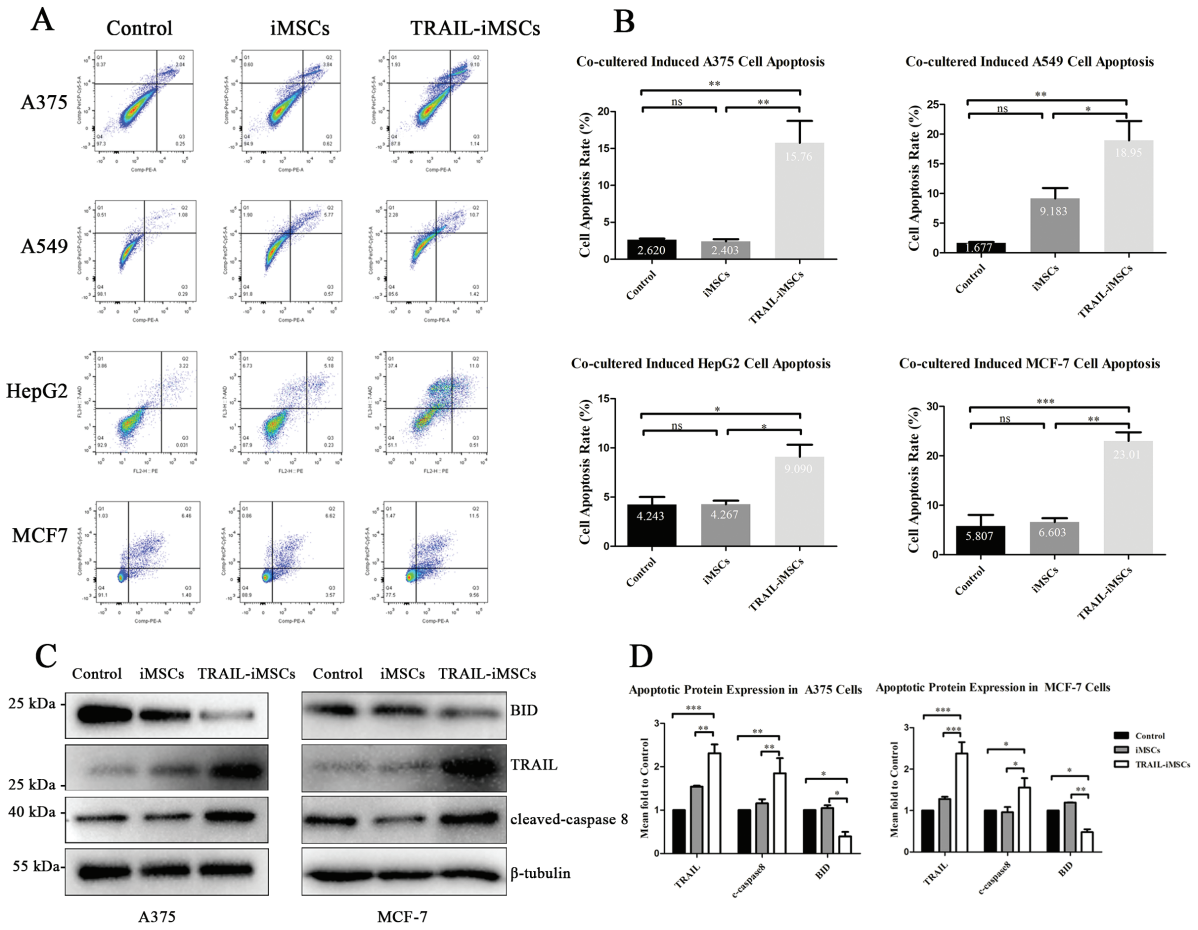

Figure 4. TRAIL-iMSCs induce cell apoptosis in vitro. (A and B) Flow cytometric analysis cell apoptosis of A375, A549, MCF-7, and HepG2. (B) Statistical analysis of total apoptosis percentage in 4 groups. Cocultured with TRAIL-iMSCs showed increased apoptosis rate compared to cocultured with iMSCs or tumor cells cultured alone in vitro (data are mean ± SEM, $n = 3$ for each group, $^{*}P < .05$, $^{**}P < .01$, $^{***}P < .001$, one-way ANOVA). (C and D) The expression of TRAIL, cleaved caspase-8 and BID were examined in A375 or MCF-7 tumor cells cultured alone (control group) and coculture with TRAIL-iMSCs or iMSCs by Western blotting analysis (data are mean ± SEM, $n = 3$ for each group, $^{*}P < .05$, $^{**}P < .01$, $^{***}P < .001$, two-way ANOVA). Abbreviations: iMSCs, induced mesenchymal stem cells; TRAIL, tumor necrosis factor-related apoptosis-inducing ligand.

human TRAIL (Supplementary Fig. S4). Notably, we detected an increased expression of TRAIL in the coculture system with TRAIL-iMSCs (Fig. 4C). Flow cytometric analysis revealed an increased rate of apoptosis in tumor cells (CFSE-negative cells) when cocultured with TRAIL-iMSCs as compared to tumor cells cultured with iMSCs or alone (Fig. 4A). The average percentage of apoptotic cells in the 4 tumor cell lines that were cocultured with TRAIL-iMSCs was increased 2-fold to 11-fold compared with the control groups (Fig. 4B).

Classically, TRAIL induces cell death via caspase-8 activation. In the present study, activated caspase-8 resulted in cleavage of pro-apoptotic protein BID into truncated BID, which translocated to the mitochondria, thereby promoting the release of cytochrome c into the cytosol and initiating the mitochondrial apoptotic pathway. The Western blotting results of A375 and MCF-7 cells showed that both procaspase-8 and BID were activated in tumor cells cocultured with TRAIL-iMSCs (Fig. 4C, 4D). However, less activation was detected when the tumor cells were cocultured with iMSCs or alone, indicating that TRAIL initiated the apoptotic pathway when cocultured with A375 or MCF-7 cells.

TRAIL-iMSCs Mediated Tumor Cell Growth Inhibition in Tumor-Bearing Mice without Toxicity

The killing ability of TRAIL-iMSCs/iMSCs was subsequently evaluated using established subcutaneous A375 and MCF-7 tumor xenografts (Fig. 5A). The growth curve of xenografts (Fig. 5C) showed that tumor growth in the TRAIL-iMSCs-treated groups was significantly suppressed, and that the average volume of the tumors formed in the TRAIL-iMSC treatment group appeared significantly smaller when compared with those formed in the iMSC treatment group and the control group (Fig. 5B) (mice without successfully established subcutaneous xenografts were excluded). Images obtained from hematoxylin and eosin-stained tumor sections confirmed that the tumor histopathology was significantly different among the 3 groups. Tumors in the untreated and iMSCs-treated groups had a relatively dense tissue structure and showed little difference in necrotic areas. In contrast, the TRAIL-iMSCs-treated group showed several necrotic areas in the tumor, as well as disrupted tumor morphology and markedly reduced tumor density with multiple, large, empty spaces in the tumor parenchyma. The necrotic/vacuolated area comprised more than 30% of the tumor sections of the TRAIL-iMSCs-treated group, which was significantly higher than

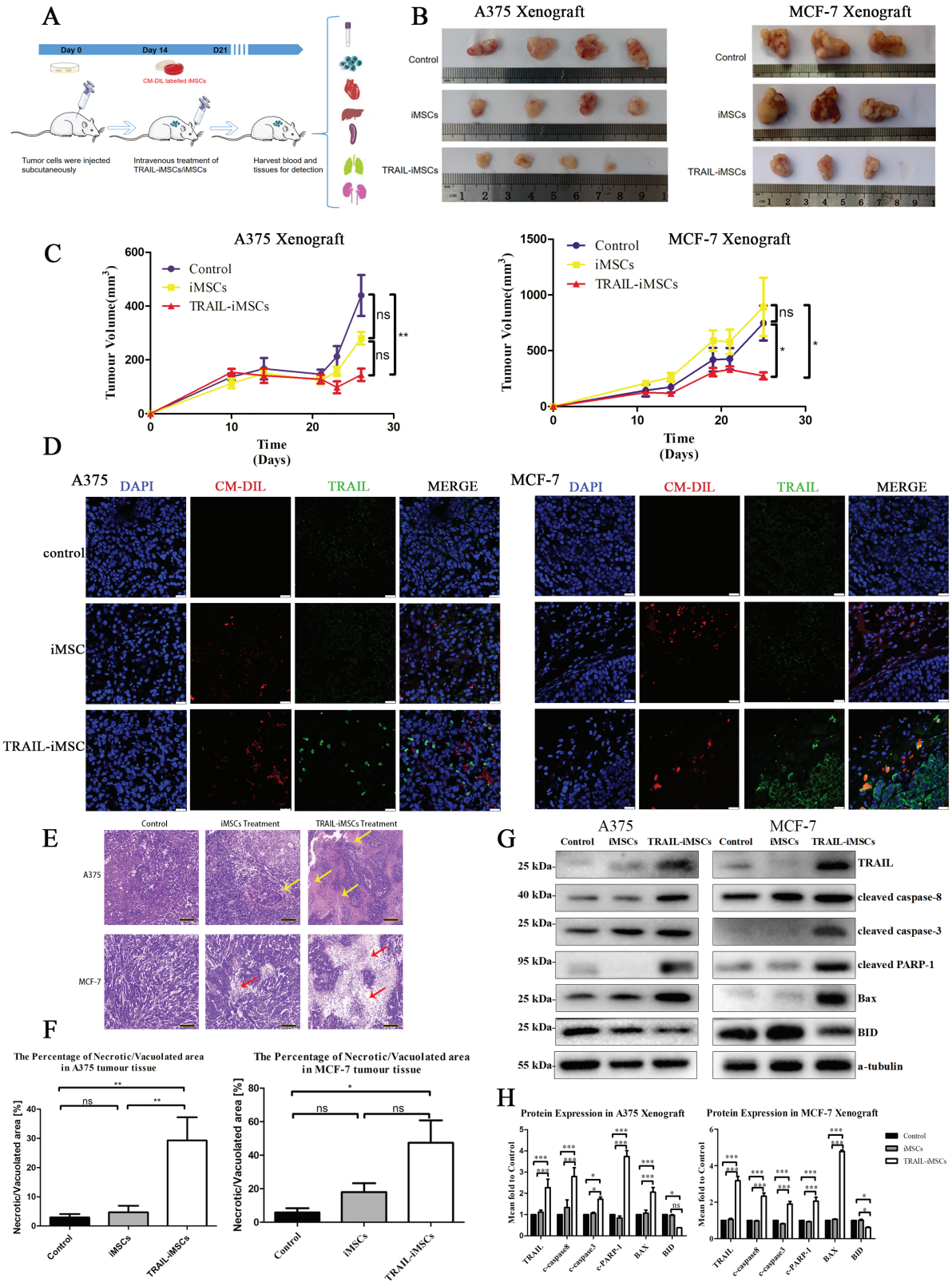

Figure 5. TRAIL-iMSCs inhibited tumor growth in xenograft models. Flow diagram of animal experiments. (B) The images of tumors were shown to compare the tumor size of each group (n = 4 per group in A375 xenografts; n = 3 per group in MCF-7 xenografts). (C) Tumor growth curve of A375 (left) and MCF-7 (right) xenograft (data are mean ± SEM, $n > 3$ for each group, $^{*}P < .05$, $^{**}P < .01$, one-way ANOVA). (D) Immunofluorescence analysis with tumor tissue sections derived from tumor xenografts. Sections examined for iMSCs/TRAIL-iMSCs with CM-Dil fluorescence (red), human TRAIL protein (green), and cell nuclei were visualized by DAPI staining (blue) (scale bar = 25 μm). (E) Histopathology of H&E-stained tumor sections from tumor-bearing mice exposed to different treatments. The yellow arrows indicate necrotic areas and red arrows point to vacuolated areas (scale bar = 200 μm). (F) The percentage of necrotic/vacuolated area in tumor tissue from H&E staining (data are mean ± SEM, n = 5 for each group, $^{*}P < .05$, $^{**}P < .01$, one-way ANOVA). (G and H) The expression levels of TRAIL and proteins related to apoptosis were examined in tumors treated with TRAIL-iMSCs, iMSCs, and untreated (control group) by Western blotting analysis. Abbreviations: DAPI, 4′,6-diamidino-2-phenylindole; iMSCs, induced mesenchymal stem cells; TRAIL, tumor necrosis factor-related apoptosis-inducing ligand.

those of the untreated and iMSCs-treated groups (Fig. 5E, 5F). Immunofluorescence analysis revealed CM-Dil-labeled TRAIL-iMSCs with intratumoral expression of TRAIL (Fig. 5D), as also observed in the iMSCs treatment group. In addition, injected TRAIL-iMSCs/iMSCs were observed mainly in the liver, spleen, and lung, but rarely in the heart and kidney (Supplementary Fig. S5).

To further demonstrate caspase cascade activation, specificity in apoptosis signaling pathways, the expression levels of apoptosis-related molecules including caspase-8, caspase-3, PARP-1, and the mitochondria-related pro-apoptotic proteins Bax and Bid were evaluated in tumor tissues (Fig. 5G, 5H). Western blotting revealed significant caspase-8 and caspase-3 activation and PARP cleavage in the TRAIL-iMSCs-treated group compared to the iMSCs treatment group and control group. We detected increased expression of Bax and activation of Bid in the TRAIL-iMSC treatment group. These results showed that the treatment of tumor-bearing mice with TRAIL-iMSCs can trigger the caspase-dependent extrinsic apoptosis pathway, which also cooperated with the intrinsic apoptosis pathway mediated by mitochondria in both A375 and MCF-7 xenografts.

Additionally, we assessed the occurrence of toxicity and other side effects during the anti-tumor process. Mice showed good health as monitored by water and food intake and behavior, and no apparent weight loss attributable to tumor burden was observed among the 3 groups (Supplementary Fig. S6). Moreover, no major systemic toxicities of the hepatic function or renal function were observed (Supplementary Table S1). These data support the anti-tumor effect of TRAIL-iMSCs and the safety of this approach in a preclinical model.

Discussion

Malignant tumors are one of the primary causes of death in humans.[23] Because of their potential to move toward the tumor site, MSCs have been engineered to express various anti-tumor factors and have shown dramatic therapeutic prospects in cancer. In this study, we attempted to find more effective and innovative therapeutic strategies that could effectively infiltrate the tumor microenvironment and deliver exogenous therapeutic agents to the tumor site. By taking advantage of previous work that efficiently integrated and expressed multiple copies of exogenous genes at the rDNA locus,[16,17] we targeted *TRAIL* to the rDNA locus using TALENickase in non-viral reprogrammed iPSCs. Then, transformed iMSCs derived from *TRAIL*-integrated iPSCs were used in vitro and in vivo to study anti-cancer effects. Our results demonstrated the possibility of inhibiting the growth of a variety of tumors by modifying human iPSC-induced MSCs to express soluble TRAIL. Compared with MSCs from conventional sources, iPSC-induced MSCs are more stable and controllable and offer other important advantages, such as rapid proliferation, virtually unlimited expandability, relatively stable phenotype, noninvasive harvesting methods, and avoidance of inter-donor variations. This work highlights a promising avenue for the development of new therapies for industrial production and clinical applications.

Viruses have been shown to be the most promising vectors for gene therapy and are widely used in cancer treatment clinical trials.[24] However, potential immune responses and unintended genomic integration events should be critically considered when viral vectors are used.[25] In previous studies, we developed a non-viral gene-targeting system mediated by TALENickase, which efficiently transferred target genes to the rDNA locus of multiple cell types, including human hepatocyte cells, MSCs, ESCs, and iPSCs.[18,26-28] Because of the multi-copy loci of the rDNA, which provided a large number of sites for homologous recombination, and the ability of TALENickases to generate less off-target mutagenesis and cytotoxicity by creating a single-strand break,[20] we efficiently targeted *TRAIL* in the rDNA locus of human iPSCs with a relative targeting efficiency of nearly 42%.

MSCs are multipotent stem cells with high differentiation potency and self-renewal ability that can be isolated from a variety of fetal and adult tissues. MSCs have been applied as cell-based drug delivery vectors for numerous clinical indications because of their ability to infiltrate the tumor stroma[29-31] with low immunogenicity.[32,33] Both naïve (unmodified) and genetically modified MSCs have been investigated for their anti-tumor effect in in vitro and in vivo cancer models. The quality of MSCs may be significantly different depending on the source. The clinical outcomes may be improved by optimizing MSC sources, and iPSC-derived MSCs have emerged as excellent candidates to address the expandability and standardization limitations of primary MSCs.[15,34] In the present study, we produced abundant iMSCs from transformed iPSCs (TRAIL-iPSCs) with high consistency. The iMSCs fulfilled the basic MSC characterization criteria proposed by the International Society for Cellular Therapy (ISCT) in 2006.[22] TRAIL-iMSCs can expand more rapidly and efficiently than primary MSCs, and they maintain the ability to continuously express the TRAIL protein while retaining their cellular characteristics. Previous studies have shown that iPSC-derived iMSCs do not promote the epithelial-mesenchymal transition, invasion, and stemness of cancer cells, as observed with bone marrow-derived MSCs.[35] Consistently, in our study, mice transplanted with A549 tumor cells mixed with TRAIL-iMSCs did not form a larger tumor than did mice transplanted with A549 alone (Supplementary Fig. S7). In addition, iPSC-iMSCs did not form teratomas in mice.[36] Numerous studies support the idea that iPSCs could be a promising source of MSCs for clinical applications.[37,38] In the future, it could be advantageous to derive genetically engineered iMSCs from iPSCs. Therefore, optimized iPSCs clones could be selected, expanded, and differentiated, thus providing a large seed bank of MSCs with uniform biological activities and/or transgene expression levels for animal experimentation and potential clinical applications.

Increasing evidence suggests that, although MSCs have an inherent capacity to migrate toward inflammation or injury sites and the tumor microenvironment,[39] chemotactic migration to specific sites is not in abundance in the case of systematic injection (unless local involvement),[40] or it is difficult for MSCs to stay in vivo long enough before clearance.[41] Therefore, it has been increasingly acknowledged that the secretion of small molecules/cytokines and exosomes/microscopic vesicles is the main mechanism of MSCs in tissue repair and anti-tumor activity.[42] Together with the results of other studies, our data confirmed that systemically injected MSCs mainly located in the lungs, liver, and spleen. This suggested that the paracrine release of TRAIL by MSCs contributes to tumor inhibition rather than direct interactions between MSCs and the tumor, which does not contradict the tissue tropism of TRAIL-iMSCs (as seen in Fig. 5D). The organ distribution and

clearance of MSCs suggest that a single MSC infusion may not be sufficient.[43]

TRAIL is a member of the TNF superfamily and exerts pro-apoptotic action on TRAIL-sensitive cancer cells with minimal effects on normal cells.[5,44] However, the clinical applications of TRAIL have been hampered by its short half-life, inadequate delivery, and treatment resistance in some cancer cell subpopulations.[45,46] Recombinant human TRAIL[45,46] and TRAIL receptor agonists[47,48] (namely, mapatumumab, conatumumab, lexatumumab, and drozitumab) have been applied in clinical trials, and modified or remodeled TRAIL proteins have also shown anti-tumor potential. Here, to improve the stability and trimerization of TRAIL, a trimer-motif isoleucine zipper was infused at the N terminus of TRAIL (aa.114-281) based on previous research results.[49] We equipped iMSCs with the soluble form of ILZ-TRAIL to generate a constant release of TRAIL into the tumor microenvironment and improve the biological activity of TRAIL. ILZ fusion endows TRAIL with high trimerization, a prolonged half-life, and low toxicity in normal cells.[49] All these efforts aimed to enhance the cytotoxic activity of TRAIL to ultimately generate apoptosis. Our results showed that genetically modified iMSCs overexpressing ILZ-TRAIL induced apoptosis in vitro and in xenograft models effectively, thereby allowing for the clinical translation of this innovative therapeutic approach.

Conclusions

In summary, we produced a steady supply of TRAIL-iMSCs from genetically modified TRAIL-iPSCs with a non-viral gene-targeting system and characterized their anti-tumor properties in vitro and in vivo. TRAIL-iMSCs induced apoptosis in A375, A549, MCF-7, and HepG2 tumor cells by activating caspase-8 and, subsequently, BID in vitro. Retro-orbital intravenous injection of TRAIL-iMSCs significantly inhibited tumor growth in A375 and MCF-7 xenograft models by triggering the caspase-dependent extrinsic apoptosis pathway and simultaneously activating the intrinsic apoptosis pathway mediated by mitochondria. Our results showed remarkable effects against multiple tumor types, thus highlighting a potential novel strategy for treating tumors based on autologous or allograft cells. Moreover, the present study revealed that integrated strategies, including gene targeting and directed differentiation of TRAIL-engineered hiPSCs, can potentially provide an unlimited number of therapeutic TRAIL-iMSCs with stable quality and high homogeneity. The results offer promise for tumor-targeted therapy and could help overcome the existing barriers to the clinical application of autologous cytotherapy in cancer.

Funding

This research was funded by the National Key Research and Development Program of China (grant number 2017YFC1001802), the National Natural Science Foundation of China (grant number 81770200), the China Postdoctoral Science Foundation (grant number 2021TQ0371), the National Key Research and Development Program of China (grant number 2016YFC0905102), and the Science and Technology Innovation Program of Hunan Province (grant number 2019SK1014).

Conflict of Interest

The authors declared no potential conflicts of interest.

Author Contribution

Z.W., H.C, G.L., P.W., and J.Z.: performed the experiments, collection, assembly, and analysis of data; G.L.: prepared the figures; Z.W.: manuscript writing, and data analysis; M.Z., Z.H., Q.H.: data analysis, manuscript writing and revision; X.L., D.L., and L.W.: concept, design, final approval of manuscript; D.L., and L.W.: funding acquisition. All authors read and approved the final manuscript.

Data Availability

All data included in this study are available upon request by contact with the corresponding author.

Supplementary Material

Supplementary material is available at *Stem Cells Translational Medicine* online.

References

1. Hmadcha A, Martin-Montalvo A, Gauthier BR, et al. Therapeutic potential of mesenchymal stem cells for cancer therapy. *Front Bioeng Biotechnol*. 2020;8:43.
2. Yin JQ, Zhu J, Ankrum JA. Manufacturing of primed mesenchymal stromal cells for therapy. *Nat Biomed Eng*. 2019;3:90-104.
3. Christodoulou I, Goulielmaki M, Devetzi M, et al. Mesenchymal stem cells in preclinical cancer cytotherapy: a systematic review. *Stem Cell Res Ther*. 2018;9:336.
4. Ashkenazi A, Pai RC, Fong S, et al. Safety and antitumor activity of recombinant soluble Apo2 ligand. *J Clin Invest*. 1999;104:155-162.
5. Walczak H, Miller RE, Ariail K, et al. Tumoricidal activity of tumor necrosis factor-related apoptosis-inducing ligand in vivo. *Nat Med*. 1999;5:157-163.
6. Dianat-Moghadam H, Heidarifard M, Mahari A, et al. TRAIL in oncology: from recombinant TRAIL to nano- and self-targeted TRAIL-based therapies. *Pharmacol Res*. 2020;155:104716.
7. Hellwig CT, Rehm M. TRAIL signaling and synergy mechanisms used in TRAIL-based combination therapies. *Mol Cancer Ther*. 2012;11:3-13.
8. Fakiruddin KS, Ghazalli N, Lim MN, et al. Mesenchymal stem cell expressing TRAIL as targeted therapy against sensitised tumour. *Int J Mol Sci*. 2018;19:2188.
9. Attar R, Sajjad F, Qureshi MZ, et al. TRAIL based therapy: overview of mesenchymal stem cell based delivery and miRNA controlled expression of TRAIL. *Asian Pac J Cancer Prev*. 2014;15:6495-6497.
10. Tang X, Lu J, Tu H, et al. TRAIL-engineered bone marrow-derived mesenchymal stem cells: TRAIL expression and cytotoxic effects on C6 glioma cells. *Anticancer Res*. 2014;34:729.
11. Loebinger MR, Eddaoudi A, Davies D, et al. Mesenchymal stem cell delivery of TRAIL can eliminate metastatic cancer. *Cancer Res*. 2009;69:4134-4142.
12. Mohr A, Lyons M, Deedigan L, et al. Mesenchymal stem cells expressing TRAIL lead to tumour growth inhibition in an experimental lung cancer model. *J Cell Mol Med*. 2008;12:2628-2643.
13. Lian Q, Zhang Y, Liang X, et al. Directed differentiation of human-induced pluripotent stem cells to mesenchymal stem cells. *Methods Mol Biol*. 2016;1416:289-298.

14. Jung Y, Bauer G, Nolta JA. Concise review: induced pluripotent stem cell-derived mesenchymal stem cells: progress toward safe clinical products. *Stem Cells*. 2012;30:42-47.
15. Sabapathy V, Kumar S. hiPSC-derived iMSCs: NextGen MSCs as an advanced therapeutically active cell resource for regenerative medicine. *J Cell Mol Med*. 2016;20:1571-1588.
16. Stults DM, Killen MW, Pierce HH, et al. Genomic architecture and inheritance of human ribosomal RNA gene clusters. *Genome Res*. 2008;18:13-18.
17. Sakai K, Ohta T, Minoshima S, et al. Human ribosomal RNA gene cluster: identification of the proximal end containing a novel tandem repeat sequence. *Genomics*. 1995;26:521-526.
18. Liu B, Chen F, Wu Y, et al. Enhanced tumor growth inhibition by mesenchymal stem cells derived from iPSCs with targeted integration of interleukin24 into rDNA loci. *Oncotarget*. 2017;8:40791-40803.
19. Wu Z, Liu W, Wang Z, et al. Mesenchymal stem cells derived from iPSCs expressing interleukin-24 inhibit the growth of melanoma in the tumor-bearing mouse model. *Cancer Cell Int*. 2020;20:33.
20. Wu Y, Gao T, Wang X, et al. TALE nickase mediates high efficient targeted transgene integration at the human multi-copy ribosomal DNA locus. *Biochem Biophys Res Commun*. 2014;446:261-266.
21. Abdal Dayem A, Lee SB, Kim K, et al. Production of mesenchymal stem cells through stem cell reprogramming. *Int J Mol Sci*. 2019;20:1922.
22. Dominici M, Le Blanc K, Mueller I, et al. Minimal criteria for defining multipotent mesenchymal stromal cells. The International Society for Cellular Therapy position statement. *Cytotherapy*. 2006;8:315-317.
23. Sung H, Ferlay J, Siegel RL, et al. Global cancer statistics 2020: GLOBOCAN estimates of incidence and mortality worldwide for 36 cancers in 185 countries. *CA Cancer J Clin*. 2021;71:209-249.
24. Bulcha JT, Wang Y, Ma H, et al. Viral vector platforms within the gene therapy landscape. *Signal Transduct Target Ther*. 2021;6:53.
25. Nayak S, Herzog RW. Progress and prospects: immune responses to viral vectors. *Gene Ther*. 2010;17:295-304.
26. Liu X, Liu M, Xue Z, et al. Non-viral ex vivo transduction of human hepatocyte cells to express factor VIII using a human ribosomal DNA-targeting vector. *J Thromb Haemost*. 2007;5:347-351.
27. Liu X, Wu Y, Li Z, et al. Targeting of the human coagulation factor IX gene at rDNA locus of human embryonic stem cells. *PLoS One*. 2012;7:e37071.
28. Hu Y, Liu X, Long P, et al. Nonviral gene targeting at rDNA locus of human mesenchymal stem cells. 2013:135189.
29. Xin H, Kanehira M, Mizuguchi H, et al. Targeted delivery of CX3CL1 to multiple lung tumors by mesenchymal stem cells. 2007;25:1618-1626.
30. Menon LG, Picinich S, Koneru R, et al. Differential gene expression associated with migration of mesenchymal stem cells to conditioned medium from tumor cells or bone marrow cells. 2007;25:520-528.
31. Chamberlain G, Fox J, Ashton B, Middleton J. Concise review: mesenchymal stem cells: their phenotype, differentiation capacity, immunological features, and potential for homing. *Stem Cells*. 2007;25:2739-2749.
32. Amorin B, Alegretti AP, Valim V, et al. Mesenchymal stem cell therapy and acute graft-versus-host disease: a review. 2014;27:137-150.
33. Almeida-Porada G, Atala AJ, Porada CD. Therapeutic mesenchymal stromal cells for immunotherapy and for gene and drug delivery. *Mol Ther Methods Clin Dev*. 2020;16:204-224.
34. Viswanathan S, Keating A, Deans R, et al. Soliciting strategies for developing cell-based reference materials to advance mesenchymal stromal cell research and clinical translation. 2014;23:1157-1167.
35. Zhao Q, Gregory CA, Lee RH, et al. MSCs derived from iPSCs with a modified protocol are tumor-tropic but have much less potential to promote tumors than bone marrow MSCs. *Proc Natl Acad Sci USA*. 2015;112:530-535.
36. Park J, Lee Y, Shin J, et al. Mitochondrial genome mutations in mesenchymal stem cells derived from human dental induced pluripotent stem cells. 2019;52:689-694.
37. Zhang W, Ge W, Li C, et al. Effects of mesenchymal stem cells from human induced pluripotent stem cells on differentiation, maturation, and function of dendritic cells. *Stem Cell Res Ther*. 2017;8:48.
38. Spitzhorn L, Megges M, Wruck W, et al. Human iPSC-derived MSCs (iMSCs) from aged individuals acquire a rejuvenation signature. *Stem Cell Res Ther*. 2019;10:100.
39. Faghih H, Javeri A, Taha MF. Impact of early subcultures on stemness, migration and angiogenic potential of adipose tissue-derived stem cells and their resistance to in vitro ischemic condition. 2017;69:885-900.
40. Spees JL, Lee RH, Gregory CA. Mechanisms of mesenchymal stem/stromal cell function. 2016;7:125.
41. Zangi L, Margalit R, Reich-Zeliger S, et al. Direct imaging of immune rejection and memory induction by allogeneic mesenchymal stromal cells. 2009;27:2865-2874.
42. Pawitan JA, Bui TA, Mubarok W, et al. Enhancement of the therapeutic capacity of mesenchymal stem cells by genetic modification: a systematic review. *Front Cell Dev Biol*. 2020;8:587776.
43. Schmuck EG, Koch JM, Centanni JM, et al. Biodistribution and clearance of human mesenchymal stem cells by quantitative three-dimensional cryo-imaging after intravenous infusion in a rat lung injury model. 2016;5:1668-1675.
44. Falschlehner C, Ganten TM, Koschny R, et al. TRAIL and other TRAIL receptor agonists as novel cancer therapeutics. 2009;647:195-206.
45. Herbst RS, Eckhardt SG, Kurzrock R, et al. Phase I dose-escalation study of recombinant human Apo2L/TRAIL, a dual proapoptotic receptor agonist, in patients with advanced cancer. *J Clin Oncol*. 2010;28:2839-2846.
46. Sayers TJ. Targeting the extrinsic apoptosis signaling pathway for cancer therapy. *Cancer Immunol Immunother*. 2011;60:1173-1180.
47. Doi T, Murakami H, Ohtsu A, et al. Phase 1 study of conatumumab, a pro-apoptotic death receptor 5 agonist antibody, in Japanese patients with advanced solid tumors. 2011;68:733-741.
48. Wakelee HA, Patnaik A, Sikic BI, et al. Phase I and pharmacokinetic study of lexatumumab (HGS-ETR2) given every 2 weeks in patients with advanced solid tumors. 2010;21:376-381.
49. Ganten TM, Koschny R, Sykora J, et al. Preclinical differentiation between apparently safe and potentially hepatotoxic applications of TRAIL either alone or in combination with chemotherapeutic drugs. 2006;12:2640-2646.